Zero-frequency current noise for the double-tunnel-junction Coulomb blockade

Selman Hershfield,* John H. Davies,† Per Hyldgaard, Christopher J. Stanton,* and John W. Wilkins

Department of Physics, 174 West 18th Avenue, The Ohio State University, Columbus, Ohio 43210
(Received 7 May 1992; revised manuscript received 3 August 1992)

We compute the zero-frequency current noise numerically and in several limits analytically for the Coulomb-blockade problem consisting of two tunnel junctions connected in series. At low temperatures over a wide range of voltages, capacitances, and resistances it is shown that the noise measures the variance in the number of electrons in the region between the two tunnel junctions. The average current, on the other hand, is linearly related to the mean number of electrons for an asymmetric pair of junctions. Thus, the noise provides additional information about transport in these devices which is not available from measuring the current alone.

I. INTRODUCTION

When the charging energy of a tunnel junction is larger than the temperature, electron tunneling events across the junction become correlated. These correlations lead to a variety of phenomena which fall under the rubric of single-electron charging effects and the Coulomb blockade[1-3] (for reviews, see Refs. 4-7). Recently, there has been renewed interest in the Coulomb blockade because of the wealth of new physical realizations: metal-insulator-metal tunnel junctions with small metal particles in the insulator,[8-10] lithographically patterned tunnel junctions,[11] scanning tunneling microscopy of small metal droplets,[12] narrow insulating wires,[13] and even thin crossed wires.[14] In some cases the technology has advanced to such an extent that one can consider making practical devices based on the Coulomb blockade.[15,4]

The theoretical work in this area has focused on the average current in either dc or ac measurements. There has been some work examining the effect of noise in the external circuit on the average current;[16] however, there have not been any studies until recently treating the current noise as an interesting phenomena in itself.[17-19] In this paper we compute the zero-frequency current noise in one of the simplest Coulomb-blockade devices consisting of two tunnel junctions connected in series. We apply the same master equation used to compute the average current.[3,20-24] This work is a direct outgrowth of an earlier paper in which we computed the noise with a similar equation which explicitly did not have charging effects.[25]

We study the zero-frequency as opposed to the finite-frequency noise because the time scale at which frequency-dependent noise begins to show structure is the "RC" charging time of the system, which is quite small ($\sim 10^{-18}$ s).[12] Noise experiments, on the other hand, are typically done in the regime below 10^5 s^{-1}. Also, because this calculation is based on the usual master equation for the Coulomb blockade, it will contain thermal noise and shot noise, but not $1/f$ noise, which is often seen in tunnel junctions at low frequencies.[26] $1/f$ noise in tunnel junctions is usually assumed to be due to defects in or near the junction. These defects are not contained in our model. Although $1/f$ noise will dominate at the lowest frequencies, there is often an intermediate regime between the very low-frequency regime and the high-frequency regime where shot noise dominates.[27] By focusing on the thermal and shot noise as opposed to the $1/f$ noise, we are able to make quantitative predictions for the noise.

The zero-frequency current noise is interesting for several reasons. First, it is a measurable effect. It may limit the accuracy of some average current measurements. There has been considerable interest recently in the zero-frequency noise in noninteracting quantum systems.[28-36] Second, we shall see that for this problem the noise provides a measure of the variance in the charge fluctuations as a function of time. The average current only provides information about the average charge between the two capacitors. Finally, the noise versus current curve has a rich structure, which is particularly revealing when rescaled by the average current. This can be used either to fit the parameters in the model more accurately or to provide a consistency check for parameters already determined from the average current. Thus, noise measurements provide an additional test for the underlying rate equation used to describe transport in this simple Coulomb-blockade device.

This paper is organized into three parts: formalism (Sec. II), analytic results (Sec. III), and numerical results (Sec. IV). In the formalism section the model and underlying master equation are reviewed, the formulas for the average current and noise are introduced, and the numerical technique used to compute the current and noise is discussed. Next, in the analytic results section, we calculate the noise in four limits: (i) the zero voltage limit, (ii) the region where the voltage is larger than the temperature but still smaller than the charging energy, (iii) the region just after the onset of current flow, and (iv) the large voltage limit. The details of the fluctuation dissipation theorem (zero voltage limit) for this system are presented in the Appendix. Finally, the noise is calculated numerically and compared to the analytic results. All the results are summarized in Sec. V.

II. FORMALISM

A. System

The system which we study consists of two tunnel junctions connected in series [see Fig. 1(a)]. The junctions are denoted L for left and R for right, and have resistances R_L and R_R and capacitances C_L and C_R, respectively. We also introduce the net resistance and capacitance of the junctions: $R = R_L + R_R$ and $C = C_L + C_R$. The charging energy of the island is $E_C = e^2/(2C)$. To drive the current a voltage V is applied to the left junction, while the voltage on the right junction is set to zero. The voltage in the central or middle region between the two junctions, V_M, fluctuates depending on the number of excess electrons in this region, n. The voltage drops across the left junction, $V_L - V_M(n)$, and the right junction, $V_M(n) - V_R$, are found using classical electrostatics to be

$$V_L - V_M(n) = \frac{C_R}{C} V + \frac{ne}{C} + V_p ,$$ (1)

$$V_M(n) - V_R = \frac{C_L}{C} V - \frac{ne}{C} - V_p .$$ (2)

Here and in all following discussions the magnitude of an electron's charge is e so that $-e$ is the electron's charge. The additional voltage V_p has been included to account for any misalignment of the Fermi level in the middle region with the Fermi levels of the left and right leads when V and n are zero.[2,24] One can also include an external gate on the central region,[24] which has a similar effect to V_p. For simplicity we omit such a gate.
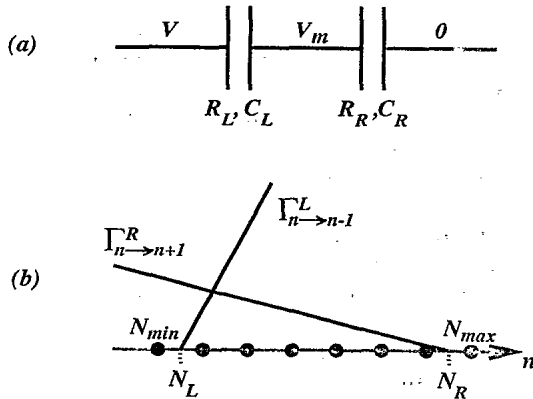

FIG. 1. Schematic of experimental geometry and rates. (a) The capacitances and resistances of the left and right junctions are (C_L, C_R) and (R_L, R_R), respectively. The voltage in the left and right leads are fixed to V and 0, respectively. The voltage in the central region, V_m, fluctuates depending on the number of electrons in the central region, n. (b) At zero temperature the rates for tunneling are linear in n. For a positive bias, $V > 0$, only the rates for tunneling onto the central region from the right lead, $\Gamma^R_{n \to n+1}$, and the rates for tunneling off the central region to the left lead, $\Gamma^L_{n \to n-1}$, are nonzero. The points where these rates vanish, N_R and N_L, determine the maximum and minimum charge states N_{max} and N_{min}.

B. Master equation

The transport through the tunnel junctions is governed by four tunneling rates: the rate for electrons to tunnel onto the central region from the left ($\Gamma^L_{n \to n+1}$) and right ($\Gamma^R_{n \to n+1}$) and the rate for electrons to tunnel off of the central region to the left ($\Gamma^L_{n \to n-1}$) and right ($\Gamma^R_{n \to n-1}$).[3,20,24] The number of excess electrons in the central region between the two junctions is n. These rates are computed via Fermi's golden rule. In order to write the rates we introduce a function $\gamma(\epsilon)$:

$$\gamma(\epsilon) = \frac{\epsilon}{1 - e^{-\beta\epsilon}} .$$ (3)

For energies ϵ larger than the temperature $k_B T$, $\gamma(\epsilon)$ is approximately ϵ, showing that the tunneling rate increases as the allowed phase space is increased. For energies ϵ less than $-k_B T$, $\gamma(\epsilon)$ is exponentially suppressed: $\gamma(\epsilon) \approx |\epsilon| e^{-\beta|\epsilon|}$, since the energy for these processes must come from thermal fluctuations. In terms of the charging energy, $E_C = e^2/(2C)$, the tunneling rates are[3,20,24]

$$\Gamma^{L(R)}_{n \to n\pm 1} = \frac{1}{e^2 R_{L(R)}} \gamma\{\pm e[V_M(n) - V_{L(R)}] - E_C\} .$$ (4)

The energies which enter the rates of Eq. (4) are the voltage drops offset by the charging energy, indicating that tunneling is suppressed for voltages smaller than the charging energy.

The state of the system at time t is described by the probability $\rho_n(t)$ that there are n electrons in the central region. Clearly the sum of the $\rho_n(t)$ is unity: $\sum_n \rho_n(t) = 1$. The time evolution of $\rho_n(t)$ is governed by the net rate, $\Gamma_{i \to j} = \Gamma^R_{i \to j} + \Gamma^L_{i \to j}$, to go from i to j excess electrons in the middle region. By incorporating the rates $\Gamma_{i \to j}$ in a matrix $\mathbf{M}$,

$$M_{ij} = \begin{cases} \Gamma_{j \to i} & \text{if } i = j \pm 1 \\ -\Gamma_{j \to j+1} - \Gamma_{j \to j-1} & \text{if } i = j \\ 0 & \text{otherwise} , \end{cases}$$ (5)

the master equation for the time evolution of $\rho(t)$ may be written succinctly as

$$\frac{d\rho(t)}{dt} = \mathbf{M}\rho(t) .$$ (6)

A direct consequence of Eqs. (5) and (6) is that the sum of the $\rho_n(t)$ is independent of time because

$$\sum_i M_{ij} = 0 .$$ (7)

Equation (7) in turn implies that the matrix $\mathbf{M}$ has a zero eigenvalue so there is a steady state solution, i.e., a vector $\rho^{(0)}$ which satisfies

$$0 = \mathbf{M}\rho^{(0)} .$$ (8)

C. Current

Although only the net transition rate $\Gamma_{i \to j}$ enters in computing $\rho(t)$, the current depends on whether an elec-

tron travels to the right or left. For example, a transition from n to $n+1$ electrons in the central region has the rate $\Gamma_{n \to n+1}$. If the additional electron tunneled from the right, this process gives a negative contribution to the number current and a positive contribution to the electrical current. On the other hand, if the additional electron tunneled from the left, there would be a positive contribution to the number current and a negative contribution to the electrical current. To take into account the difference in sign for the two processes, we introduce two new matrices, v^L and v^R, which contain the rates for tunneling across the left and right junctions, respectively. The sign of a matrix element is positive if a process gives a positive contribution to the number current from left to right, and negative if a process gives a negative contribution to the number current.

$$v_{ij}^{L(R)} = \begin{cases} -(+)\Gamma_{j \to i}^{L(R)} & \text{if } i = j-1 \\ +(-)\Gamma_{j \to i}^{L(R)} & \text{if } i = j+1 \\ 0 & \text{otherwise .} \end{cases} \quad (9)$$

With these definitions the electrical current across the left (I_L) and right (I_R) junctions at time t are

$$I_{L(R)}(t) = -e \sum_i [v^{L(R)}\rho(t)]_i$$

$$\equiv -e \, \text{Tr}\{v^{L(R)}\rho(t)\} . \quad (10)$$

In Eq. (10), we have defined a trace of a vector to be the sum of its elements. Both the currents I_L and I_R are positive when the electrical current goes from left to right. To obtain the steady-state current from Eq. (10), $\rho(t)$ is replaced by $\rho^{(0)}$.

In general the current in the left and right junctions will be different; however, in the zero-frequency limit they must be the same because of the continuity equation. To derive the continuity equation we introduce the number matrix N, where $N_{ij} = i \times \delta_{ij}$. The expectation value for the number of electrons in the central region at time t is

$$N(t) = \text{Tr}\{N\rho(t)\} . \quad (11)$$

Using the rate equation for the probability, Eq. (6), the time derivative of $N(t)$ is

$$\frac{dN(t)}{dt} = \text{Tr}\{NM\rho(t)\} . \quad (12)$$

The key observation is that $v^L - v^R$ is the commutator of N and M.

$$v^L - v^R = [N, M] . \quad (13)$$

Using Eqs. (7) and (13), the time derivative of the charge in the central region may be written as

$$-e\frac{dN(t)}{dt} = -e \, \text{Tr}\{[N,M]\rho(t)\} = I_L(t) - I_R(t) , \quad (14)$$

which is the continuity equation. As noted above in the steady state, $dN(t)/dt = 0$, and I_L is equal to I_R.

D. Noise

To define the noise we introduce the propagator $P(t)$, which gives the time evolution of $\rho_n(t)$:

$$P(t) = \exp(Mt) . \quad (15)$$

The conditional probability that there are m electrons in the middle region, given that there were n electrons at $t=0$, is $P_{m,n}(t)$. It is understood that t is positive in Eq. (15). With $P(t)$ we can compute all possible correlation functions between the density and the current.[37,38] For example, the density-density correlation function is

$$\langle N(t)N(0) \rangle = \theta(t)\text{Tr}\{NP(t)N\rho^{(0)}\}$$

$$+ \theta(-t)\text{Tr}\{NP(-t)N\rho^{(0)}\} . \quad (16)$$

This equation has a simple physical interpretation. Initially, the probability distribution is the steady-state solution $\rho^{(0)}$. The number of the electrons in the central region is measured by N at this initial time. Next, the system is propagated forward in time via P, and the number is again measured with N. For $t>0$ the initial time is $t=0$ and the final time is t, while for $t<0$ the initial time is t and the final time is 0. In a similar manner the density-current correlation function is ($A = R$ or L)

$$\langle N(t)I_A(0) \rangle = -e\theta(t)\text{Tr}\{NP(t)v^A\rho^{(0)}\}$$

$$-e\theta(-t)\text{Tr}\{v^A P(-t)N\rho^{(0)}\} . \quad (17)$$

The only difference between Eqs. (17) and (16) is that the matrix v^A measures the current across one of the junctions instead of the number of electrons in the central region measured by N.

In analogy with Eqs. (16) and (17), the current-current correlation function should have two matrices v^A and v^B for measuring current at the two times 0 and t. Although such a term includes the correlation between two different tunneling events, it does not include the self-correlation of a given tunneling event with itself. In our earlier paper[25] we gave a formal derivation of the self-correlation term as well as the correlation between different tunneling events. Here we insert this self-correlation term by hand. Suppose there is a current pulse across the right junction between 0 and dt. The number current is $(dt)^{-1}$ during the time interval dt, and the number current squared is $(dt)^{-2}$. The probability of this happening is dt times the average number current to the right. Thus, it would seem that the self-correlation term for $\langle I_R(t)I_R(0) \rangle$ is just $eI\delta(t)$. However, the current can be either positive or negative, and the self-correlation term is always positive. Thus, in computing the self-correlation term we must take the absolute value of the matrix elements of v^L and v^R used in computing the current. These new matrices may be written succinctly as $([N, v^L])_{i,j} = |(v^L)_{i,j}|$ and $([v^R, N])_{i,j} = |(v^R)_{i,j}|$. Thus, the current-current correlation function is ($A, B = R$ or L)

$$\langle I_A(t)I_B(0)\rangle = e^2\theta(t)\text{Tr}\{\mathbf{v}^A \mathbf{P}(t)\mathbf{v}^B \rho^{(0)}\}$$
$$+ e^2\theta(-t)\text{Tr}\{\mathbf{v}^B \mathbf{P}(-t)\mathbf{v}^A \rho^{(0)}\}$$
$$\pm\delta_{A,B=\{^L_R\}}e^2\delta(t)\text{Tr}\{[\mathbf{N},\mathbf{v}^A]\rho^{(0)}\} \ . \tag{18}$$

The first two lines of this equation contain the correlation between two different tunneling events, while the last line is the self-correlation term.

As for the average current, the continuity equation identity Eq. (13) can be used to show that any occurrence of $(I_L - I_R)$ may be replaced by $-e(dN/dt)$.

$$-e\frac{d}{dt}\langle N(t)N(0)\rangle = \langle [I_L(t)-I_R(t)]N(0)\rangle \ , \tag{19}$$

$$-e\frac{d}{dt}\langle N(t)I_A(0)\rangle = \langle [I_L(t)-I_R(t)]I_A(0)\rangle \ . \tag{20}$$

In the zero-frequency limit this implies that both the current-current correlation function and the current-density correlation functions are independent of where the current is measured. The noise $S_{AB}(\omega)$ is now defined as the Fourier transform of the current-current correlation function, $\langle I_A(t)I_B(0)\rangle$, with its long-time behavior subtracted.

$$S_{AB}(\omega) = 2\int_{-\infty}^{\infty} dt \, e^{i\omega t}[\langle I_A(t)I_B(0)\rangle - \langle I\rangle^2] \ . \tag{21}$$

The continuity equation [Eq. (20)] and the relation $S_{AB}(\omega)=S_{BA}(-\omega)$ imply that correlation functions for all possible choices of $A,B=R,L$ are equal in the zero-frequency limit, $\omega=0$. As discussed in the Introduction, we will always be taking the zero-frequency limit because it is the easiest to study experimentally.

E. Numerical technique

In order to compute the noise it is useful to symmetrize the matrix **M**. The key observation is that this system obeys detailed balance [see Eq. (8)]:

$$\Gamma_{i\to j}\rho_i^{(0)} = \Gamma_{j\to i}\rho_j^{(0)} \ . \tag{22}$$

A direct consequence of Eq. (22) is that $M_{ij}\rho_j^{(0)}=M_{ji}\rho_i^{(0)}$, allowing us to define a symmetric matrix $\overline{\mathbf{M}}$,

$$\overline{M}_{ij} \equiv \sqrt{\rho_j^{(0)}/\rho_i^{(0)}}M_{ij} = \sqrt{M_{ij}M_{ji}} \ . \tag{23}$$

In a similar manner we define $\overline{\mathbf{v}}^A$ as $(\rho_j^{(0)}/\rho_i^{(0)})^{1/2}\mathbf{v}^A$ and $\overline{\rho}_i^{(0)}$ as the square root of $\rho_i^{(0)}$, so that the expectation values may also be written in a symmetric form, e.g.,

$$\mathbf{I_A} = -e\overline{\rho}^{(0)}\overline{\mathbf{v}}^A\overline{\rho}^{(0)} \ . \tag{24}$$

The matrix $\overline{\mathbf{M}}$ is written in terms of its eigenvalues, $\lambda \le 0$, and eigenvectors, x_λ, as

$$\overline{M}_{ij} = \sum_\lambda \lambda(x_\lambda)_i(x_\lambda)_j \ . \tag{25}$$

Using this same representation, the noise $S_{AB}(\omega)$ is given by

$$S_{AB}(\omega) = 2e^2 \sum_{\lambda\neq 0} (\overline{\rho}^{(0)}\overline{\mathbf{v}}^A x_\lambda)\frac{1}{-\lambda-i\omega}(x_\lambda\overline{\mathbf{v}}^B\overline{\rho}^{(0)})$$
$$+ 2e^2 \sum_{\lambda\neq 0} (\overline{\rho}^{(0)}\overline{\mathbf{v}}^B x_\lambda)\frac{1}{-\lambda+i\omega}(x_\lambda\overline{\mathbf{v}}^A\overline{\rho}^{(0)})$$
$$\pm\delta_{A,B=\{^L_R\}}2e^2(\overline{\rho}^{(0)}[\mathbf{N},\overline{\mathbf{v}}^A]\overline{\rho}^{(0)}) \ . \tag{26}$$

In this paper we truncate the matrix $\overline{\mathbf{M}}$ to include some finite number of states and then diagonalize it to determine its eigenvalues and eigenvectors. The eigenvector with zero eigenvalue is $\overline{\rho}^{(0)}$. Equations (24) and (26) are used to compute the current and noise.

III. LIMITS

Before discussing the results of our numerical evaluation of the zero-frequency noise, in this section we compute the noise in four limits which may be treated analytically. The cases discussed are: (A) the zero voltage limit, where the noise is related to the conductance via the fluctuation dissipation theorem; (B) the thermally activated conduction regime, where the voltage drop is large compared to the temperature but still small compared to the charging energy; (C) the two-state region, where the voltage is larger than the charging energy but small enough that only two charge states are allowed; and (D) the large voltage bias limit.

A. Zero voltage

Even though we will focus on potential drops eV, large compared to the thermal energy $k_B T$, any technique for computing the noise must reproduce the fluctuation dissipation theorem[39,40] at zero bias:

$$S = 4k_B TG(V=0) \ , \tag{27}$$

where G is the differential conductance, $G=\partial I/\partial V$. In the Appendix we show how Eq. (27) follows from the definitions of the rates [Eq. (4)] and the expression for the noise [Eq. (26)]. In Sec. IV we also verify that our numerical algorithm produces the fluctuation dissipation theorem at zero bias.

B. Thermally activated conduction

When the voltage is large compared to the temperature, the thermal noise is small compared to the shot noise, which comes from the current flowing. Even with $e|V| \gg k_B T$, if the voltage is small compared to charging energy, the conduction is thermally activated because the voltage drop alone does not provide enough energy to overcome the charging energy.[41] In this section we show that in this regime $(E_C \gg e|V| \gg k_B T)$ the noise is related to the current by the standard shot-noise relation

$$S = 2e|I| \ . \tag{28}$$

In this limit the steady-state probability distribution function $\rho_n^{(0)}$ is strongly peaked about one value of n except for special values of V_p where two states are equally occupied. We shall assume that we are not at one of

these special points and call the state which is most likely occupied the $n=0$ state. To describe the transport it is sufficient to keep only three states: the $n=0$ state and the two states immediately accessible from this state: $n=\pm 1$. At $T=0$ the matrix $\mathbf{M}$ thus becomes

$$\mathbf{M}(T=0)=\begin{bmatrix} -\Gamma_{-1\to 0} & 0 & 0 \\ \Gamma_{-1\to 0} & 0 & \Gamma_{1\to 0} \\ 0 & 0 & -\Gamma_{1\to 0} \end{bmatrix}. \tag{29}$$

The eigenvector of $\mathbf{M}(T=0)$ with zero eigenvalue is (0, 1, 0), indicating that at zero temperature only $\rho_{n=0}^{0}$ is nonzero. For a finite temperature there is a small correction $\delta\mathbf{M}\equiv\mathbf{M}-\mathbf{M}(T=0)$, which allows transitions to the states $n=\pm 1$.

$$\delta\mathbf{M}=\begin{bmatrix} -\delta\Gamma_{-1\to 0} & \delta\Gamma_{0\to -1} & 0 \\ \delta\Gamma_{-1\to 0} & -\delta\Gamma_{0\to 1}-\delta\Gamma_{0\to -1} & \delta\Gamma_{1\to 0} \\ 0 & \delta\Gamma_{0\to 1} & -\delta\Gamma_{1\to 0} \end{bmatrix}. \tag{30}$$

There are analogous zero-temperature and finite-temperature correction terms for $\mathbf{v}^{L}$ and $\mathbf{v}^{R}$.

Because we have reduced $\mathbf{M}$ to a 3×3 matrix, Eqs. (24) and (26) for the current and noise can easily be expanded to linear order in the $\delta\Gamma$'s:

$$\frac{I}{e}=\left[\frac{\Gamma_{1\to 0}^{L}}{\Gamma_{1\to 0}}\delta\Gamma_{0\to 1}^{R}+\frac{\Gamma_{-1\to 0}^{R}}{\Gamma_{-1\to 0}}\delta\Gamma_{0\to -1}^{L}\right]$$
$$-\left[\frac{\Gamma_{1\to 0}^{R}}{\Gamma_{1\to 0}}\delta\Gamma_{0\to 1}^{L}+\frac{\Gamma_{-1\to 0}^{L}}{\Gamma_{-1\to 0}}\delta\Gamma_{0\to -1}^{R}\right], \tag{31}$$

$$\frac{S}{2e^2}=\left[\frac{\Gamma_{1\to 0}^{L}}{\Gamma_{1\to 0}}\delta\Gamma_{0\to 1}^{R}+\frac{\Gamma_{-1\to 0}^{R}}{\Gamma_{-1\to 0}}\delta\Gamma_{0\to -1}^{L}\right]$$
$$+\left[\frac{\Gamma_{1\to 0}^{R}}{\Gamma_{1\to 0}}\delta\Gamma_{0\to 1}^{L}+\frac{\Gamma_{-1\to 0}^{L}}{\Gamma_{-1\to 0}}\delta\Gamma_{0\to -1}^{R}\right]. \tag{32}$$

These equations have a simple physical interpretation. Conduction in this thermally activated regime follows from the occurrence of a rare transition from $n=0$ to $n=\pm 1$, followed by a rapid decay back into the $n=0$ state. Thus, for example, there could be a thermal fluctuation causing an electron to tunnel from the right lead to the central region ($\delta\Gamma_{0\to 1}^{R}$). This thermal fluctuation is followed shortly by the electron tunneling off to the right lead ($\Gamma_{1\to 0}^{R}$) or to the left lead ($\Gamma_{1\to 0}^{L}$). If an electron tunnels to the right lead then there is no contribution to the current, while if the electron tunnels to the left lead there is a positive contribution to the electrical current. Thus, only a fraction of the time, $\Gamma_{1\to 0}^{L}/\Gamma_{1\to 0}$, does this thermally activated process contribute to the current. This explains the first term in Eq. (31): $(\Gamma_{1\to 0}^{L}/\Gamma_{1\to 0})\delta\Gamma_{0\to 1}^{R}$. The other terms in this equation have similar interpretations.

The noise in this regime only contains the self-correlation term because we have independent thermally activated processes which are separated by long periods in time. Thus, the only difference between the current

and the noise is one sign change resulting from some processes giving a negative contribution to the current and a positive self-correlation term for the noise. Dividing Eq. (32) by Eq. (31), it would seem that their ratio is not $2e$; however, because the voltage is large compared to the temperature, two of the activated rates are always much larger than the other two. For $I>0$, $\delta\Gamma_{0\to 1}^{R}$ and $\delta\Gamma_{0\to -1}^{L}$ are much larger than $\delta\Gamma_{0\to 1}^{L}$ and $\delta\Gamma_{0\to -1}^{R}$ by a factor exponential in $e|V|/k_{B}T$, while for $I<0$ the situation is reversed. Therefore, the noise is indeed equal to $2e$ times the absolute value of the current [Eq. (28)].

C. Two-state regime

Eventually the voltage becomes larger than the charging energy, and there is current flow even at zero temperature. As discussed above, in the thermally activated regime only one charge state is allowed at zero temperature. At the onset of nonthermally activated current flow, there are two allowed charge states at $T=0$, except for the special case of a symmetric pair of junctions, where there are three allowed charge states. We only consider the asymmetric case here. It is a good approximation to keep only these two states for some range in temperature, $k_{B}T\ll E_{C}$. Our two-state approximation is similar but not identical to the one used in Ref. 42. They compute $\rho^{(0)}$ using only two states, and then allow transitions to a third state in computing the current [Eq. (24)]. We do not allow transitions to a third state; however, in the regime of interest here, where only two states are energetically accessible, the two approaches give the same result for the current.

Since only two states are involved, there are only two rates. In the case $I>0$ one rate Γ^{R}, increases the number of electrons by tunneling across the right junction, while the other rate Γ^{L} decreases the number of electrons by tunneling across the left junction. These rates depend on the voltage drop across the sample and can be determined from Eqs. (3) and (4). In the next section we will also give the limiting form of these rates at zero temperature. Since $\mathbf{M}$ in this limit is a 2×2 matrix,

$$\mathbf{M}=\begin{bmatrix} -\Gamma^{R} & \Gamma^{L} \\ \Gamma^{R} & -\Gamma^{L} \end{bmatrix}, \tag{33}$$

it is simple to solve for the current and the noise:

$$I=e\frac{\Gamma^{L}\Gamma^{R}}{\Gamma^{L}+\Gamma^{R}}\bigg|_{V}, \tag{34}$$

$$S=2eI\frac{(\Gamma^{R})^2+(\Gamma^{L})^2}{(\Gamma^{R}+\Gamma^{L})^2}\bigg|_{V}. \tag{35}$$

We wish to emphasize here that although Eqs. (34) and (35) look simple, they contain a great deal of structure because the rates Γ^{L} and Γ^{R} depend on voltage. This will be shown explicitly in Sec. IV, when we plot this result along with the numerical results for finite temperatures. From Eqs. (34) and (35), we can see that I is largest when two rates are equal. Also, the noise is suppressed from its uncorrelated value $S=2e|I|$. This suppression is to be

expected because having only two allowed states in the central region introduces correlations between tunneling events. If the system is at one of the allowed states, say the state with more electrons, then another electron cannot tunnel onto the central region until an electron tunnels off. This kind of correlation did not appear in the thermally activated regime, because an electron tunnels off so quickly after tunneling on that it has no effect on subsequent tunneling events.

D. High-voltage limit

We have now computed the noise for $V=0$, $E_C \gg e|V| \gg k_B T$, and $e|V| \gtrsim E_C$. In this section we compute the noise for $e|V| \gg E_C$, where we expect the current-voltage characteristic to be almost linear. Even though we compute the noise in the asymptotic high-voltage limit, in Sec. IV we will see some of the approximations derived here work down to $e|V| \sim E_C$.

Because we are interested in the limit where the voltage is larger than the other energy scales, $k_B T$ and E_C, we set the temperature equal to zero. This means that $\gamma(\epsilon)$ in Eq. (3) takes on a very simple form: $\gamma(\epsilon) = \epsilon\theta(\epsilon)$. If the sample is biased so that the electrical current flows from left to right, then two kinds of processes are important at $T=0$: tunneling across the right junction to the central region ($\Gamma^R_{n \to n+1}$) and tunneling from the central region to the left lead ($\Gamma^L_{n \to n-1}$). The rates for these processes are

$$\Gamma^L_{n \to n-1} = \frac{1}{R_L C}(n - N_L)\theta(n - N_L) , \quad (36)$$

$$\Gamma^R_{n \to n+1} = \frac{1}{R_R C}(N_R - n)\theta(N_R - n) , \quad (37)$$

where the numbers N_L and N_R are given by

$$N_L = -\frac{C_R V}{e} - \frac{C V_p}{e} + \frac{1}{2} \quad (38)$$

$$N_R = \frac{C_L V}{e} - \frac{C V_p}{e} - \frac{1}{2} \quad (39)$$

These rates are illustrated in Fig. 1(b). The minimum allowed state $N_{\min}$ is the largest value of n for which $(n - N_L) < 0$. Similarly, the maximum allowed state $N_{\max}$ is the smallest n for which $(N_R - n) < 0$. Assuming that $N_L < 0$ and $N_R > 0$, this means that the values of n with $\rho^0_n \neq 0$ are

$$N_{\min} = -\text{Int}(-N_L - 1) \le n \le \text{Int}(N_R + 1) = N_{\max} . \quad (40)$$

Since I_R and I_L are just the expectation values of $\Gamma^R_{n \to n+1}$ and $\Gamma^L_{n \to n-1}$, respectively, it is tempting to call Eqs. (36) and (37) with $n \to \langle n \rangle$ the current. This is not correct because $\Gamma^L_{n \to n-1} = (n - N_L)/(R_L C)$ is only valid for $n \ge N_{\min} + 1$. For $n = N_{\min}$ the rate $\Gamma^L_{n \to n-1}$ is zero. Similarly, $\Gamma^R_{n \to n+1} = (N_R - n)/(R_R C)$ is only valid for $n \le N_{\max} - 1$. However, in the limit $R_L \ll R_R$ the rate for tunneling across the left junction, $\Gamma^L_{n \to n-1}$, is much larger than the rate for tunneling across the right junction, as illustrated in Fig. 1(b). This means that $\langle n \rangle$ is

close to $N_{\min}$. Because $\rho^{(0)}_{N_{\max}} \approx 0$, it is then a good approximation to replace n by $\langle n \rangle$ in Eq. (37):

$$I \approx e\frac{1}{R_R C}(N_R - \langle n \rangle) . \quad (41)$$

In a similar manner for $R_R \ll R_L$, the probability of being in the state $n = N_{\min}$ is small and we can approximate the current by Eq. (36) with $n \to \langle n \rangle$:

$$I \approx e\frac{1}{R_L C}(\langle n \rangle - N_L) . \quad (42)$$

Equations (41) and (42) show that the current is linearly related to the average number of electrons in the middle region for an asymmetric pair of junctions.

Up to this point we have not made any assumptions about the voltage being much larger than the charging energy. Now we assume that N_L and N_R are integers. This can only be true for a limited set of voltages; however, in the large voltage limit the current and noise should be insensitive to whether N_L and N_R are integers. We verify this numerically in Sec. IV by showing that the results predicted here are asymptotically true in the high-voltage limit.

If N_L and N_R are integers, then we have shown in our earlier paper[25] that the noise can be computed exactly (see also Chen and Ting[43]). The current can also be computed exactly in this special case.[37,44,45] Here we review the results in the context of this problem. For integers N_L and N_R the number electrons in the middle region, $N(t)$, satisfy a simple rate equation

$$\frac{dN(t)}{dt} = \frac{N_R - N(t)}{R_R C} - \frac{N(t) - N_L}{R_L C} . \quad (43)$$

This allows one to compute both the steady-state current

$$I = \frac{e}{RC}\left[\frac{CV}{e} - 1\right] \quad (44)$$

and to relate the zero-frequency noise to the variance in the number of electrons in the middle region, var(n),

$$S = 2eI - \frac{4e^2}{RC}\text{var}(n) . \quad (45)$$

The variance of n is given by

$$\text{var}(n) = \frac{R_L^{-1}R_R^{-1}}{(R_L^{-1} + R_R^{-1})^2}\left[\frac{CV}{e} - 1\right] , \quad (46)$$

so the noise in the high-voltage limit is

$$S = 2eI\frac{R_L^{-2} + R_R^{-2}}{(R_L^{-1} + R_R^{-1})^2} . \quad (47)$$

Note the formal similarity of these results with those of the two-state regime [Eqs. (34) and (35)]. An important difference between these two sets of results is that R_L^{-1} and R_R^{-1} are constant, while Γ^L and Γ^R depend on voltage. Thus, here $S/2eI$ goes to a constant asymptotic value, while before $S/2eI$ depended on voltage. In the next section we will show numerically that Eq. (47) is

indeed valid in the high-voltage limit, and Eq. (45) is a good approximation for much smaller voltages.

IV. NUMERICAL RESULTS

In this section we present the results for computing the noise and current via Eqs. (24) and (26). There are six parameters in the model besides the voltage: the resistances R_L and R_R, the capacitances C_L and C_R, the temperature T, and the offset voltage V_p. Two of these parameters can be eliminated by rescaling the rates by $R = R_R + R_L$ and the energies by the charging energy $E_C = e^2/2C$. Thus, our parameter space consists of the resistance ratio R_L/R, the capacitance ratio C_L/C, the temperature divided by the charging energy $k_B T/E_C$, and eV_p/E_C. In evaluating Eqs. (24) and (26) we will always truncate the matrix **M** because the higher charge states $|n| \gg 1$ are energetically forbidden, especially at low temperatures and voltages. In practice we have found it is sufficient to keep the 15 states surrounding $n = 0$. With this many states the steady-state solution $\rho_n^{(0)}$ is zero to within our numerical accuracy for the highest $(n = 7)$ and lowest states $(n = -7)$. Increasing the number of states does not change $\rho_n^{(0)}$.

A. Temperature dependence

For most of this section we will consider temperatures far below the charging energy because this is where charging effects are most important. To start, however, we set the voltage equal to zero and verify that our numerical algorithm satisfies the fluctuation dissipation theorem [Eq. (27)]. In Fig. 2, we have plotted both the noise S and the differential conductance $G = dI/dV$ as a function of temperature for a pair of junctions with $R_L/R = 0.01$ and $C_L/C = 0.01$. As expected in a
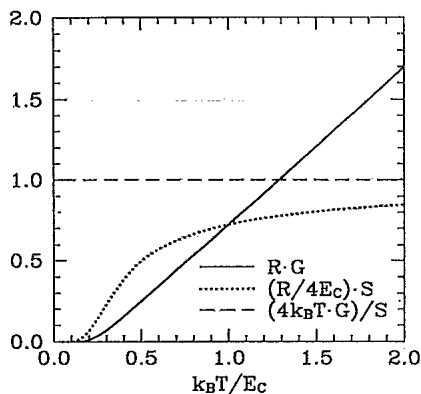
Coulomb-blockade problem, the conductance and noise are suppressed for temperatures much less than the charging energy ($\lesssim 0.2E_C$, here). For temperatures greater than or of the order of the charging energy, the conductance rises linearly with temperature, indicating that the number of accessible states is increasing with temperature. In this same regime the noise approaches a constant value as required by the fluctuation dissipation theorem. We have divided the two curves to show explicitly that the fluctuation dissipation theorem is satisfied.

B. Dependence on V_p

In Fig. 3, the current and noise versus voltage curves are plotted for $CV_p = 0$ and $CV_p = 0.25$. The temperature is much less than the charging energy, $k_B T = 0.01E_C$. As expected for an asymmetric pair of junctions with $R_L = 0.01R$ and $C_L = 0.01C$, the curves exhibit the step-like structure of the Coulomb staircase. The primary effect of the offset V_p is to shift the I-V and S-V curves. To reduce the parameter space in subsequent plots we will specialize to $V_p = 0$, where the I-V and S-V characteristics are symmetric in the voltage. In this figure the fact that the noise and current curves are almost the same indicates that the noise is close to its uncorrelated value: $S = 2eI$. Careful examination shows that the noise is actually less than $2eI$. The amount by which it is less than $2eI$ changes as a function of voltage. Thus, in subsequent plots we will also look at the noise ratio $S/2eI$ to bring out this structure.

C. Dependence on the capacitance and resistance ratios

Restricting ourselves to $k_B T \ll E_C$ and $V_p = 0$, the parameter space becomes two dimensional: $(R_L/R_R, C_L/C_R)$ or $(R_L/R, C_L/C)$. It is well known that for asymmetric junctions with $R_L \ll R_R$ and $C_L \ll C_R$ (or
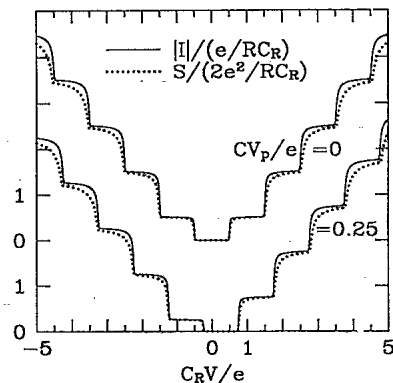

FIG. 2. The equilibrium noise S and conductance $G = dI/dV$ for two tunnel junctions connected in series. At temperatures far below the charging energy of the tunnel junctions, $E_C = e^2/2C$, both the conductance (solid curve) and the zero-frequency noise (dotted curve) are suppressed by the Coulomb blockade. At temperatures above the charging energy the conductance is roughly linear in temperature and the noise approaches a constant value. In accordance with the fluctuation dissipation theorem the ratio of the noise to the conductance remains fixed at $4k_B T$ (see dashed curve).

FIG. 3. The nonequilibrium noise and current. At low temperatures $(k_B T = 0.01E_C)$ for an asymmetric junction $(R_L/R = 0.01$ and $C_L/C = 0.01)$ both the average current I and the noise S show the characteristic step structure of the Coulomb staircase. Indeed, S is roughly equal to the standard shot noise result of $2eI$. With an offset voltage V_p the current-voltage and noise-voltage characteristics are shifted, but other qualitative features of the curves remain the same. Henceforth we set $V_p = 0$.

$R_L \gg R_R$ and $C_L \gg C_R$) the Coulomb-staircase structure as in Fig. 3 is seen, while for asymmetric junctions with $R_L \ll R_R$ and $C_L \gg C_R$ (or $R_L \gg R_R$ and $C_L \ll C_R$) no steplike structure is seen. There is only a suppression of the current for small voltages.

The noise ratio $S/2eI$ vs the current curves are the new contribution of this paper. The first observation to make about these curves is that there is a rich variety of structure in the noise when rescaled by the current. This structure is not contained in the current. For example, one might say that the $S/2eI$ curves in Fig. 5 are simply related to the derivative of the current; however, there is no simple way to take the derivative of the current curves in Fig. 4 and obtain the $S/2eI$ curves in that figure.
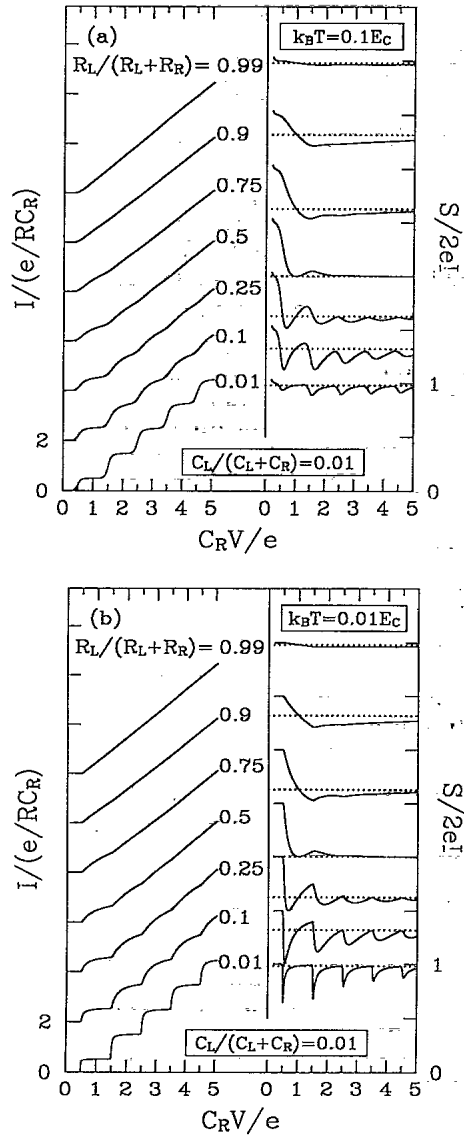

FIG. 4. The dependence of the current and noise ratio $(S/2eI)$ on the resistances of the junctions at (a) $k_B T = 0.1 E_C$ and (b) $k_B T = 0.01 E_C$. We go from good steps $(C_L/C = 0.01, R_L/R = 0.01)$ to no steps $(C_L/C = 0.01, R_L/R = 0.99)$ by varying the resistance ratio R_L/R_R, keeping the capacitances fixed at $C_L/C = 0.01$ and $C_R/C = 0.99$. When the difference between S and I illustrated in Fig. 3 is plotted as the noise ratio, $S/2eI$, a rich variety of structure is revealed. This structure becomes more pronounced as one goes down in temperature. The noise ratio shows structure even when the current shows little structure, illustrating how the noise can provide new information about the parameters in the model. The dotted lines are the asymptotic value of the noise ratio at large voltages [Eq. (47)]. Since the noise remains finite as the current goes to zero, the noise ratio diverges as $V \to 0$. We have thus only plotted it for $C_R V/e > 0.2$. [This is the reason $S/2eI > 1$ at low voltages in (a).]
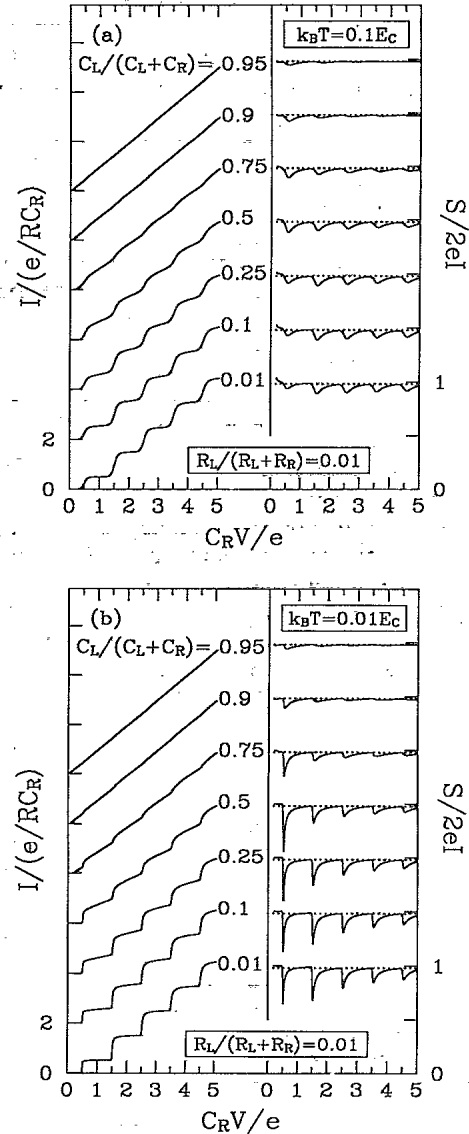

FIG. 5. The current and noise ratio as a function of the capacitance ratio at (a) $k_B T = 0.1 E_C$ and (b) $k_B T = 0.01 E_C$. $(R_L/R = 0.01)$ Varying the capacitance instead of the resistance has a different effect. All the noise ratio curves have a similar structure, indicating that the noise is more sensitive to the resistance ratio than capacitance ratio. This should not be too surprising because the asymptotic limit of the noise ratio (dotted lines) is determined by the resistances of the junctions [see Eq. (47)]. Although the abscissas of Fig. 4 and this figure are the same, the voltage ranges are different because the capacitances vary here.

Using the structure in $S/2eI$, one can determine the parameters in the model more accurately than one could with the current alone. Alternately, one can use the parameters obtained from the current to perform a consistency check. We illustrate this point by considering three examples from Figs. 4 and 5. In Fig. 4(b), the top three cases, $R_L/R =0.75$, 0.9, and 0.99, have almost identical current-voltage characteristics, yet their noise-ratio curves are quite distinguishable. As a second example, the steps in the $R_L/R =0.5$ I-V curve are only slightly more pronounced than the steps in the $R_L/R =0.75$ curve; however, the noise-ratio curves exhibit a change in curvature. The upper curve has a downward cusp, while the lower curve has an upward cusp. Finally, we note that the $R_L/R =0.1$ curve in Fig. 4(b) and the $C_L/(C_L +C_R)=0.25$ or 0.5 curves in Fig. 5(b) are quite similar, although their noise-ratio curves are very different.

Comparing Fig. 4(a) to 4(b) and Fig. 5(a) to 5(b), there is considerable sharpening in the noise-ratio curves as one goes down in temperature. The spiky structure of the curves in Fig. 5(b) $(k_B T=0.01E_C)$ is just beginning to be visible in Fig. 5(a) $(k_B T=0.1E_C)$. It is natural to ask whether even $T=0.01E_C/k_B$ is the zero-temperature limit. For the higher voltages and less asymmetric junctions, one has indeed reached the zero-temperature limit, i.e., the curves do not change appreciably as one goes down in temperature; however, the lower voltage regions of the more asymmetric junctions continue to become sharper as one goes down in temperature. To illustrate this we have plotted in Fig. 6 the region around the first
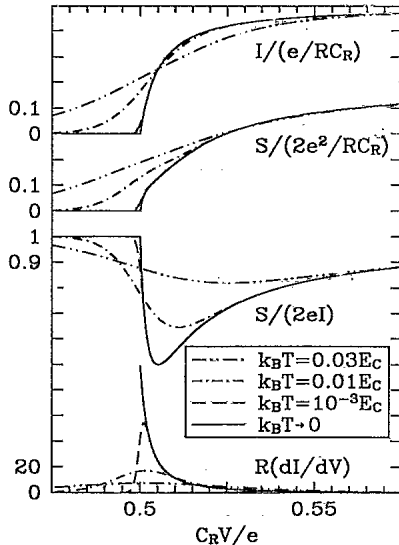

FIG. 6. The temperature dependence for the most asymmetric junctions shown in Figs. 4 and 5 ($R_L/R =0.01$, $C_L/C =0.01$). The current (I), the noise (S), the noise ratio ($S/2eI$), and the differential conductance ($G=dI/dV$) all show significant temperature dependence below $k_B T=0.01E_C$. The spiky structure in the noise ratio is due to a combined effect of I and S having sharper structure as one goes to lower temperatures. The zero-temperature curves are obtained from the analytic expressions for the noise in the two state limit [Eqs. (34) and (35)].

step in the most asymmetric junction of Figs. 4 and 5 ($C_L =0.01C$, $R_L =0.01R$) for four temperatures. The $T\rightarrow 0$ curves were computed analytically using the two-state approximation of Sec. III C. For all of the curves shown, I, S, $S/2eI$, and dI/dV, there is significant enhancement of the structure for temperatures below one-one-hundredth of the charging energy. Both the current and the noise become sharper as one goes down in temperature, showing that the increased structure in the noise ratio is a combination of effects in the noise and current.

D. Discussion of the noise ratio

While the above shows that the noise provides new information about the transport in these systems, it does not give us a simple interpretation of what this information means. In this section we use the analytic results of Sec. III, to understand our numerical results. Three limits are discussed: the thermally activated regime before the first step; the region just after the first step, where the two-state approximation is valid; and the large voltage limit, where the current and noise-voltage characteristics become linear. We also test an approximate formula for the noise which interpolates between the high- and low-voltage limits. This formula relates the zero-frequency noise to the variance in the number of electrons in the middle region. All these cases except for the very high-voltage limit are presented in Fig. 7. The asymptotic large voltage limit is illustrated in Figs. 4 and 5.

The first region we consider is the thermally activated regime where the voltage drop is much smaller than the temperature. In Sec. III B we showed that in this region $S/2eI$ is unity at sufficiently low temperatures because the current flows in one direction via rare uncorrelated events. In Figs. 4 and 5 we do indeed find that the noise ratio is unity in the low-voltage regime below the first step in the I-V characteristic. This is shown more explicitly in Fig. 7, where we replot the solid curves of Figs. 4(b) and 5(b) along with several analytic approximations, shown as solid dots. In Fig. 7(a) the thermally activated regime extends up to $C_R V/e =0.5$ (region I). Because the capacitance ratios vary in Fig. 7(b), the extent of the thermally activated regime also varies. For $C_R >C_L$ the thermally activated regime extends up to $C_R V/e =\frac{1}{2}$, while for $C_L >C_R$ it extends up to $C_R V/e =(\frac{1}{2})(C_R /C_L)$. Thus, the thermally activated regime for the top curve in this figure only extends up to $C_R V/e =0.5(0.05/0.95)\approx 0.026$. We have not put in any solid dots for the thermally activated regime in Fig. 7(b) to avoid cluttering the graph. In both of these figures the noise ratio is not shown down to zero voltage because at any finite temperature ($k_B T=0.01E_C$ here) thermal fluctuations cause $S/2eI$ to diverge as $V\rightarrow 0$.

For an asymmetric pair of junctions the region just above the thermally activated regime in Fig. 7 is the two-state limit. In this regime only two states have nonzero occupation probability. If the system is in one state, then the only allowed transition is to the other state. This introduces correlations which in turn suppress the noise. For the processes in the thermally ac-

tivated regime, there were also two relevant rates: one slow rate due to thermal activation, and a quick decay rate from the excited state. Because one of the rates was much longer than the other, the problem reduced to one
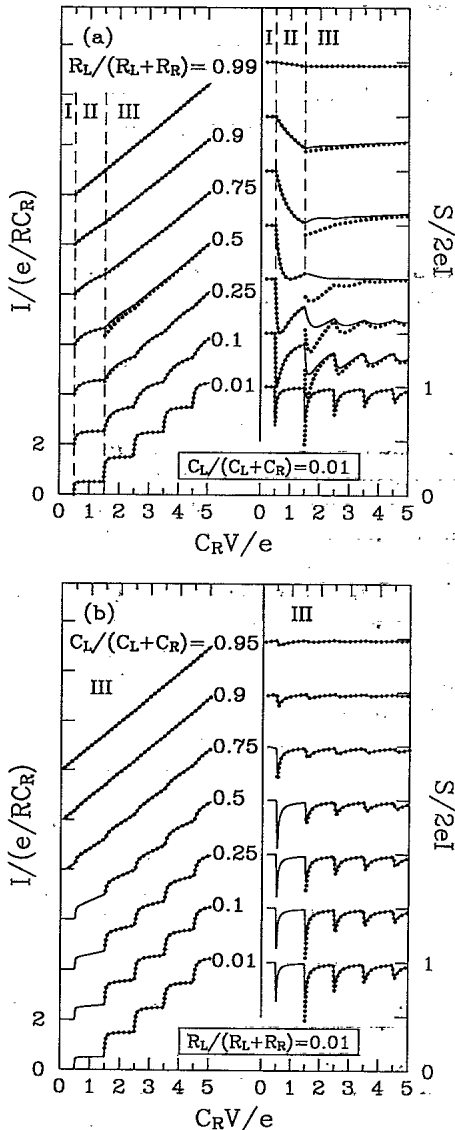

FIG. 7. Approximations for the current and the noise. The solid lines are the numerical results of Figs. 4(b) and 5(b), and the dots are the approximations. (a) In the thermally activated regime labeled by I the noise ratio is unity. In the two-state regime labeled by II the current and noise are given by Eqs. (34) and (35). Both this and the thermally activated regime are exact at low temperatures. In the higher voltage regime, region III, we have used Eqs. (41) $[R_L \leq R_R]$ and (42) $[R_R \leq R_L]$ and Eq. (45), which relate the current and noise to the mean and variance in the number of electrons in the region between the two tunnel junctions. Although these approximations are not exact, they clearly indicate the important qualitative features of the current and noise. (b) With this abscissa the boundaries of the thermally activated and two-state regimes vary as one changes the capacitances. Thus, although the thermally activated and two-state regimes are also exact here, we have only shown the large voltage approximation to avoid cluttering the graph.

with just the slow rate. Another way to say this is that the noise in the two-state limit, $S = 2eI[(\Gamma^L)^2 + (\Gamma^R)^2]/(\Gamma^L + \Gamma^R)^2$ [Eq. (35)], reduces to classical shot noise $S = 2eI$ when one of the rates is much larger than the other.

In Figs. 7(a) and 7(b), one of the rates is much smaller than the other near the onset, and the noise ratio is close to unity. As the voltage is increased the smaller rate increases and the noise is suppressed. In this regime the maximum possible suppression is $\frac{1}{2}$ when $\Gamma^R = \Gamma^L$. In Fig. 7(a) most of the curves in the two-state regime (region II) do indeed go down to $\frac{1}{2}$. The curves then return up as the rate which was originally smaller now becomes the larger rate. The exceptions are the $R_L = 0.01R$ and $C_L = 0.01C$ junction, which has not yet reached the zero-temperature limit (see Fig. 6), and the three upper curves, where the smaller rate does not reach the larger rate before the next step. In Fig. 7(b) the same physics holds, but we have not illustrated the two-state regime with solid dots because the place where the two-state regime is valid varies with C_L/C.

It is tempting to say that our two-state approximation for the noise works even after the first step, especially for asymmetric junctions where the probability is strongly peaked about either the maximum or minimum allowed state. While the strictly two-state approximation predicts the qualitative features of the noise-ratio voltage curves for higher-order steps, it is not quantitative. In particular we can see from Figs. 4 and 5 that the noise ratio does not go down to $\frac{1}{2}$ after the first step. Our two-state approximation predicts that the noise goes down to $\frac{1}{2}$ for the higher steps as well. Rather than try to extend the two-state approximation by, for example, including three states, we now turn to the large voltage limit.

In Sec. III D we argued that in the large voltage limit the noise ratio should be given by $S/2eI = (R_L^{-2} + R_R^{-2})/(R_L^{-1} + R_R^{-1})^2$ [Eq. (47)]. This expression is remarkably similar to the expression we found in the two-state limit for the noise ($\Gamma_{L(R)} \to R_{L(R)}^{-1}$); however, it is important to keep in mind that the high-voltage limit is definitely not a limit where the two-state approximation is valid. Rather, formulas with this structure appear in a wide variety of contexts, including both quantum coherent[32,34] and incoherent transport.[36,25] We regard them as a ubiquitous but not universal high-voltage limit when only two rates are important. To check this asymptotic limit, the dotted lines in Figs. 4 and 5 (not Fig. 7) are the ratio in Eq. (47). Clearly, it is approached at large biases.

This still leaves the intermediate regime, where more than two states are important and one has not reached the asymptotic limit of large voltages. From Eqs. (41) $[R_L \leq R_R]$ and (42) $[R_R \leq R_L]$, we see that at least for asymmetric junctions the current provides a measure of the mean number of electrons in the central region. In region III of Figs. 7(a) and 7(b), the solid dots over the numerical I-V characteristics show that these expressions are good approximations for the current even for the less asymmetric junctions. Since the current provides a measure of the mean number of electrons in the middle re-

gion, $\langle n \rangle$, it is natural to try to express the current fluctuations in terms of the variance of n, var(n). In deriving the high-voltage limit, we found that $S = 2eI - 4e^2 \mathrm{var}(n)/(RC)$ [Eq. (45)]. The solid dots in region III in Fig. 7(a) and all the solid dots in Fig. 7(b) are the noise ratio computed with this approximation using the numerically determined var(n). Although this is not as good an approximation as for the current, it works remarkably well down to lower voltages. The reductions in the noise can be regarded as an increase in the variance, which is to be expected near a step where there are large fluctuations. The places where the approximation works most poorly, e.g., $R_L/R = 0.5$ and 0.75 in Fig. 7(a), are also the places where the approximation for the current works worst. This last approximation for the noise provides us with the simple intuitive picture that the noise measures the variance in n while the current gives information about the mean.

V. CONCLUSION

In this paper we have computed the zero-frequency current noise for the simple Coulomb-blockade problem consisting of two tunnel junctions connected in series. The noise was computed both numerically and analytically using the same master equation as for the current. The numerical results are exact within the context of the master equation. The analytic results were shown to agree with the numerical results in four regimes: the zero voltage limit, the thermally activated regime, the region where only two charge states are accessible at low temperatures, and the large voltage limit. The low-temperature limit in some cases is not obtained until the temperature is very much less than E_C, e.g., $k_B T = 10^{-3} E_C$. For the intermediate-voltage regime we obtained a useful approximation to the noise which related the noise to the variance in the number of electrons in the region between the tunnel junctions. Thus, while the current for an asymmetric pair of junctions is linearly related to the mean number of electrons in this region, the noise measures the variance.

Both the numerical and analytic results showed that the noise contains information which is not contained in the current. Thus, by measuring the zero-frequency noise we can determine the five parameters in the model more accurately than one could with the current alone. Alternately, one can use the noise to check the results obtained by measuring the current, showing possible deficiencies in the underlying rate equation used to describe transport in this system.

ACKNOWLEDGMENTS

APPENDIX

The proof of the fluctuation dissipation theorem in quantum mechanics is a few lines long. On the other hand, the proof for most classical systems is much longer. In this appendix we prove the fluctuation dissipation theorem in two steps. We first simplify the expression for the noise in equilibrium and then simplify the expression for the linear response conductance.

1. Simplified expression for the noise

Since we are interested in the zero-frequency noise, we define a new matrix, $\delta \mathbf{P}$,

$$\delta P_{ij} = \int_0^\infty dt [P_{ij}(t) - \rho_i^{(0)}] . \tag{A1}$$

As can be seen by applying $\mathbf{M}$ to Eq. (A1), δP_{ij} is related to the inverse of $\mathbf{M}$:

$$(\mathbf{M}\delta\mathbf{P})_{ij} = \rho_i^{(0)} - \delta_{ij} . \tag{A2}$$

The zero-frequency noise may be expressed directly in terms $\delta \mathbf{P}$:

$$S_{AB} = 2e^2 \mathrm{Tr}\{v^A \delta \mathbf{P} v^B \rho^{(0)}\} + 2e^2 \mathrm{Tr}\{v^B \delta \mathbf{P} v^A \rho^{(0)}\}$$
$$\pm \delta_{A,B=\{^L_R\}} 2e^2 \mathrm{Tr}\{[\mathbf{N}, v^A]\} . \tag{A3}$$

In equilibrium the matrices v^L and v^R are proportional to one another. We thus define a matrix v which satisfies $v^R = -R_R^{-1}v$, $v^L = R_L^{-1}v$, and

$$v = \frac{1}{R_L^{-1} + R_R^{-1}}[\mathbf{N}, \mathbf{M}] . \tag{A4}$$

Equation (A4) allows us to reduce Eq. (A3) to two different kinds of traces: $\mathrm{Tr}\{[\mathbf{N},[\mathbf{N},\mathbf{M}]]\rho^{(0)}\}$ and $\mathrm{Tr}\{[\mathbf{N},\mathbf{M}]\delta\mathbf{P}[\mathbf{N},\mathbf{M}]\rho^{(0)}\}$. These traces can be simplified using: (i) the trace of $\mathbf{M}$ times any vector is zero [Eq. (7)], (ii) $\mathbf{M}\rho^{(0)}$ is zero [Eq. (8)], and (iii) $\mathbf{M}\delta\mathbf{P}$ is related to the identity matrix via Eq. (A2). The end result is that the noise in equilibrium is

$$S = -4e^2 \frac{R_L^{-1} R_R^{-1}}{(R_L^{-1} + R_R^{-1})^2} \mathrm{Tr}\{\mathbf{N}\mathbf{M}\mathbf{N}\rho^{(0)}\} . \tag{A5}$$

2. Simplified expression for the linear-response conductance

In equilibrium the probability function $\rho_n^{(0)}$ has a thermal distribution, i.e., it is the exponential of $-\beta$ times some energy E_n. The simplest way to see this is to use the detailed balance [Eq. (22)]

$$\frac{\Gamma_{n\to n-1}}{\Gamma_{n-1\to n}} = \frac{\rho_{n-1}^{(0)}}{\rho_n^{(0)}} = \frac{e^{-\beta E_{n-1}}}{e^{-\beta E_n}} , \tag{A6}$$

where the energy E_n is

$$E_n = \frac{e^2 n^2}{2C} + eV_p n . \tag{A7}$$

The fact that the distribution is thermal and that E_n is given by Eq. (A7) allows one to express the derivative of

$\rho^{(0)}$ with respect to V_p in terms of the equilibrium probability

$$\frac{\partial \rho_n^{(0)}}{\partial V_p} = -\beta e(n - \mathrm{Tr}\{\mathbf{N}\rho^{(0)}\}\rho_n^{(0)}) \ . \tag{A8}$$

The strategy now is to express partial derivatives with respect to V in terms of partial derivatives with respect to V_p. At the end we use Eq. (A8) to rewrite partials with respect to V_p in terms of equilibrium expectation values. Because we know that the currents I_L and I_R are equal, we will only consider I_L. The quantity which we are computing is the linear-response conductance

$$\frac{\partial I}{\partial V} = -e \, \mathrm{Tr}\left\{\frac{\partial \mathbf{v}^L}{\partial V}\rho^{(0)}\right\} - e \, \mathrm{Tr}\left\{\mathbf{v}^L\frac{\partial \rho^{(0)}}{\partial V}\right\} , \tag{A9}$$

where this and all other partial derivatives are evaluated at $V=0$. The derivative of I with respect to V_p at $V=0$ is zero because I at $V=0$ is zero.

$$\frac{\partial I}{\partial V_p} = -e \, \mathrm{Tr}\left\{\frac{\partial \mathbf{v}^L}{\partial V_p}\rho^{(0)}\right\} - e \, \mathrm{Tr}\left\{\mathbf{v}^L\frac{\partial \rho^{(0)}}{\partial V_p}\right\} = 0 \ . \tag{A10}$$

Because the Γ^L's are functions of $C_R V + CV_p$, derivatives with respect to V can be related to ones with respect to V_p.

$$\frac{\partial \mathbf{v}^L}{\partial V} = \frac{C_R}{C}\frac{\partial \mathbf{v}^L}{\partial V_p} \ . \tag{A11}$$

Using Eqs. (A9)–(A11), one partial derivative with respect to V can be eliminated:

$$\frac{\partial I}{\partial V} = -e \, \mathrm{Tr}\left\{\mathbf{v}^L\left[\frac{\partial \rho^{(0)}}{\partial V} - \frac{C_R}{C}\frac{\partial \rho^{(0)}}{\partial V_p}\right]\right\} \ . \tag{A12}$$

In order to eliminate the other derivative with respect to V, we note that $\mathbf{M}\rho^{(0)}$ is zero for all voltages, and hence

$$\frac{\partial \mathbf{M}}{\partial V}\rho^{(0)} + \mathbf{M}\frac{\partial \rho^{(0)}}{\partial V} = 0 \ , \tag{A13}$$

$$\frac{\partial \mathbf{M}}{\partial V_p}\rho^{(0)} + \mathbf{M}\frac{\partial \rho^{(0)}}{\partial V_p} = 0 \ . \tag{A14}$$

As in Eq. (A11), we can relate derivatives with respect to V to derivatives with respect to V_p:

$$\frac{\partial \mathbf{M}}{\partial V} = \frac{R_L^{-1}C_R - R_R^{-1}C_L}{C(R_L^{-1} + R_R^{-1})}\frac{\partial \mathbf{M}}{\partial V_p} \ . \tag{A15}$$

Using Eqs. (A13)–(A15), the linear-response conductance is

$$\frac{\partial I}{\partial V} = e\frac{R_L^{-1}R_R^{-1}}{(R_L^{-1} + R_R^{-1})^2}\mathrm{Tr}\left\{\mathbf{N}\mathbf{M}\frac{\partial \rho^{(0)}}{\partial V_p}\right\} \ . \tag{A16}$$

As our final simplification of dI/dV, we use Eq. (A8) to convert the partial with respect to V_p to traces involving $\rho^{(0)}$.

$$\frac{\partial I}{\partial V} = -\beta e^2\frac{R_L^{-1}R_R^{-1}}{(R_L^{-1} + R_R^{-1})^2}\mathrm{Tr}\{\mathbf{N}\mathbf{M}\mathbf{N}\rho^{(0)}\} \ . \tag{A17}$$

Dividing Eq. (A5) by Eq. (A17), we obtain the fluctuation dissipation theorem, Eq. (27).

---

*Permanent address: Department of Physics, University of Florida, Gainesville, FL 32611.

†Permanent address: Department of Electronics and Electrical Engineering, University of Glasgow, Glasgow G12 8QQ, UK.

[1]H. R. Zeller and I. Giaever, Phys. Rev. **181**, 789 (1969).

[2]J. Lambe and R. C. Jaklevic, Phys. Rev. Lett. **22**, 1371 (1969).

[3]O. Kulik and R. I. Shekhter, Zh. Eksp. Teor. Fiz. **68**, 623 (1975) [Sov. Phys. JETP **41**, 308 (1975)].

[4]K. K. Likharev, IBM J. Res. Dev. **32**, 144 (1988).

[5]D. V. Averin and K. K. Likharev, in *Mesoscopic Phenomena in Solids*, edited by B. Altshuler *et al.* (Elsevier, New York, 1991).

[6]G. Schon and A. D. Zaikin, Phys. Rep. **198**, 237 (1990).

[7]*Single Charge Tunneling*, edited by H. Grabert and M. Devoret, Vol. 294 of *NATO Advanced Study Institute, Series B* (Plenum, New York, 1992).

[8]J. B. Barner and S. T. Ruggiero, Phys. Rev. Lett. **59**, 807 (1987).

[9]L. S. Kuz'min and K. K. Likharev, Pis'ma Zh. Eksp. Teor. Fiz. **45**, 389 (1987) [JETP Lett. **45**, 495 (1987)].

[10]P. J. M. van Bentum, T. T. M. Smokers, and H. van Kempen, Phys. Rev. Lett. **60**, 2543 (1988).

[11]D. A. Fulton and G. J. Dolan, Phys. Rev. Lett. **59**, 109 (1987).

[12]R. Wilkins, E. Ben-Jacob, and R. C. Jaklevic, Phys. Rev. Lett. **63**, 801 (1989).

[13]V. Chandrasekhar, Z. Ovadyahu, and R. A. Webb, Phys. Rev. Lett. **67**, 2862 (1991).

[14]S. Gregory, Phys. Rev. Lett. **64**, 689 (1990).

[15]L. J. Geerligs *et al.*, Phys. Rev. Lett. **64**, 2691 (1990).

[16]A. N. Cleland, J. M. Schmidt, and J. Clarke, Physica B **165&166**, 979 (1990).

[17]G. Zimmerli, T. M. Eiles, H. D. Jensen, R. L. Kautz, and J. M. Martinis, Bull. Am. Phys. Soc. **37**, 764 (1992).

[18]J. W. Wilkins, S. Hershfield, J. H. Davies, P. Hyldgaard, and C. Stanton, Phys. Scr. **T42**, 115 (1992).

[19]A. N. Korothov, D. V. Averin, K. K. Likharev, and S. A. Vasenko, in *Single Electron Tunneling and Mesoscopic Devices*, edited by H. Koch and H. Luebbig, Springer Series in Electronics and Photonics Vol. 31 (Springer-Verlag, Berlin, 1992), p. 45.

[20]K. Mullen, E. Ben-Jacob, R. C. Jaklevic, and Z. Schuss, Phys. Rev. B **37**, 98 (1988).

[21]Yu. V. Nazarov, Pis'ma Zh. Eksp. Teor. Fiz. **49**, 105 (1989) [JETP Lett. **49**, 126 (1989)].

[22]M. Devoret *et al.*, Phys. Rev. Lett. **64**, 1824 (1990).

[23]S. Girvin *et al.*, Phys. Rev. Lett. **64**, 3183 (1990).

[24]M. Amman, R. Wilkins, E. Ben-Jacob, P. D. Maker, and R. C. Jaklevic, Phys. Rev. B **43**, 1146 (1991).

[25]J. H. Davies, P. Hyldgaard, S. Hershfield, and J. W. Wilkins, Phys. Rev. B **46**, 9620 (1992).

[26]C. T. Rogers and R. A. Buhrman, Phys. Rev. Lett. **53**, 1272 (1984).

[27]Y. P. Li, A. Zaslavsky, D. C. Tsui, M. Santos, and M. Shayegan, Phys. Rev. B **41**, 8388 (1990).

[28]G. B. Lesovik, Pis'ma Zh. Eksp. Teor. Fiz. **49**, 513 (1989) [JETP Lett. **49**, 592 (1989)].

[29]V. A. Khlus, Zh. Eksp. Teor. Fiz. **93**, 2179 (1987) [Sov. Phys. JETP **66**, 1243 (1987)].

[30]R. Landauer, Physica (Amsterdam) D **38**, 226 (1989).

[31]B. Yurke and G. P. Kochanski, Phys. Rev. B **41**, 8184 (1990).

[32]M. Buttiker, Phys. Rev. Lett. **65**, 2901 (1990); Physica **175**, 199 (1991); Phys. Rev. Lett. **68**, 843 (1992).

[33]R. Landauer and Th. Martin, Physica **175**, 167 (1991).

[34]L. Y. Chen and C. S. Ting, Phys. Rev. B **43**, 534 (1991).

[35]C. W. J. Beenakker and X. van Houten, Phys. Rev. B **43**, 12066 (1991).

[36]C. W. J. Beenakker and M. Buttiker, Phys. Rev. B **46**, 1889 (1992).

[37]For a review, see K. M. van Vliet and J. R. Fassett, in *Fluctuation Phenomena in Solids,* edited by R. E. Burgess (Academic, New York, 1965), p. 267.

[38]For a discussion in the context of tunneling, see R. Landauer, J. Appl. Phys. **33**, 2209 (1962).

[39]J. B. Johnson, Phys. Rev. **29**, 367 (1927).

[40]H. Nyquist, Phys. Rev. **32**, 229 (1928).

[41]For the special case that two charge states are equally likely to be occupied in equilibrium the current flow is not thermally activated for small voltages.

[42]J.-C. Wan, K. A. McGreer, L. I. Glazman, A. M. Goldman, and R. I. Shekhter, Phys. Rev. B **43**, 9381 (1991).

[43]L. Y. Chen and C. S. Ting, Phys. Rev. B **46**, 4714 (1992).

[44]B. Laikhtman, Phys. Rev. B **43**, 2731 (1991).

[45]H. Grabert *et al.,* Z. Phys. B **84**, 143 (1991).